International Journal on
"Technical and Physical Problems of Engineering"
(IJTPE)
Published by International Organization of IOTPE

ISSN 2077-3528
IJTPE Journal
www.iotpe.com
ijtpe@iotpe.com

March 2022 | Issue 50 | Volume 14 | Number 1 | Pages 57-63

OPTIMAL FOTID CONTROLLER DESIGN FOR REGULATION OF DC MOTOR SPEED

R. Mohajery H. Shayeghi P. Zare

Energy Management Research Center, University of Mohaghegh Ardabili, Ardabil, Iran
rezamohajery76@gmail.com, hshayeghi@gmail.com, eps.peymanzare@gmail.com

Abstract- Owing to the critical role of DC motors in industrial systems, utilizing economical and accurate methods to control motor speed is essential. This article presents an optimized Fractional-order TID (FOTID) controller to regulate DC motor speed using slime mould algorithm. The proposed algorithm produces more excellent results and uses less processing time than other algorithms. Moreover, in the process of designing and evaluating the performance of controllers, a time-domain performance index called the ISTSE is defined as the objective function, and ISE and ITSE are determined as evaluation functions. The performance of the FOTID controller is studied by applying torque changes in the presence of parametric uncertainties under various scenarios than the FOPID and TID controllers. The performance of the suggested method in terms of response speed, reduction of overshoot, rise time and settling time is shown. Analysis of the results indicates that the speed control method with the FOTID controller works significantly better than the FOPID and TID ones.

Keywords: Slime Mold Algorithm, DC Motors, FOTID Controller, TID Controller.

1. INTRODUCTION

DC motors are often utilized in industries due to their simple design and employed in automobiles, electric vehicles, robotics, automation, etc. It is a mechanical energy converter that transforms electrical energy into mechanical energy. In general, the motor speed is proportional to the applied voltage. It has an inverse relation with the generated magnetic flux, and the rotor speed changes by changing the armature voltage or field current [1].

Researchers developed various control methods with different controllers to regulate the speed of DC motors [2]. Different structures of the classical controllers based on Proportional-Integral-Derivative Controller (PID) and different optimization algorithms such as Harris Hawk's Optimizer (HHO) [3], Atom Search (ASO) [4], the Grey Wolf Optimization (GWO) [5] and Teaching Learning-Based Optimization (TLBO) [6] were introduced in recent studies. Furthermore, the speed of a DC motor has been controlled using an Artificial Neural Network Technique (ANN) [7], which aims to control the speed of the rotor even with the noise. It should be noted that this technique, like other methods, has benefits and drawbacks. Although the system's performance increased by a controller using the artificial neural network technique, the critical issue is the long training time and selection of layers and neurons in each layer.

In a DC control loop, a fractional-order PID controller named FOPID has been discussed to analyze the motor speed [8]. The experimental findings indicated that the FOPID controller exceeds the PID controller in the overall performance and efficiency if correctly designed and implemented. Furthermore, implementing a fuzzy PI controller based on a genetic algorithm to regulate the speed of a DC motor showed the effectiveness of the recommended controller compared to the conventional PI controller [9]. Additionally, to achieve the minimum settling time in DC motor speed control, an improved version of the whale optimization algorithm (IWOA) was used to correctly choose the PID controller coefficients [10].

Due to the nonlinear properties of the DC motor and design constraints, accurate speed control cannot be accomplished with the classical controllers. Therefore, this article proposes a novel FOTID controller structure to regulate the speed of a DC motor. The proposed FOTID controller allows for enhanced disturbance rejection and increased sensitivity to changes in system parameters. Hence, it functions better than other related controllers like PID and FOPID ones. In regulating the DC motor speed, the slime mold optimization algorithm (SMA) [11] used to optimize the suggested controller coefficients. This method has a high convergence speed compared to other meta-heuristic algorithms and has an adequate performance in discovering excellent solutions and not getting stuck in the local optimization. In addition, the proposed algorithm provides a better response in most scenarios and is an efficient technique to establish stability in the speed control process when system uncertainty occurs.

In summary, this research aims to achieve higher performance than previous techniques by using a novel controller and a high-precision algorithm. Moreover, the error between the reference and the exact speed is

optimized by minimizing the objective function. Finally, the proposed model of DC motor is simulated in MATLAB/Simulink software under various scenarios.

The following is a summary of the article's six parts. Section II discusses the fundamental features of the DC motor model. Section III provides a brief explanation of the FOTID controller's structure. The objective function and SMA algorithm theories are discussed in Sections IV and V. In section VI, a modified DC motor with FOTID, FOPID, and TID controllers is simulated, and the results are displayed.

2. DESCRIPTION OF A DC MOTOR

DC motors are mainly divided into two classes of external and self-excited. This article analyzes an externally excited DC motor to regulate the speed by armature voltage control. Figure 1 illustrates the speed control circuit model for the DC motor system, and Table 1 displays its parameters.

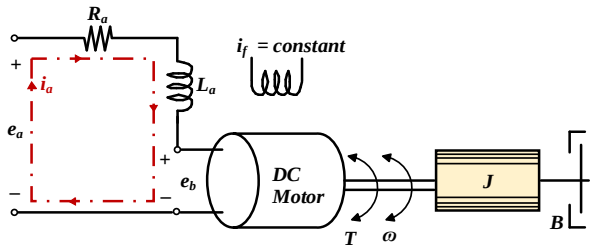

Figure 1. The speed control circuit model for the DC motor

Table 1. DC motor system parameters

Symbol	Parameter	Unit
R_a	resistance of the armature	Ω
L_a	inductance of the armature	H
i_a	current of the armature	A
i_f	field current	A
e_a	applied armature voltage	V
e_b	back electromotive force	V
T	torque of the motor	N.m
ω	motor shaft angular speed	rad/s
J	motor inertia torque	Kg.m^2
K_b	constant of electromotive force	V.s/rad
K	constant torque of the motor	N.m/A
B	motor friction constant	N.m.s/rad

The induced voltage (e_b) has a connection with the angular velocity as follows:

$$e_b = K_b \frac{d\theta}{dt} = K_b \omega \tag{1}$$

The armature voltage (e_a) controls the speed of a DC motor. Therefore, the armature circuit's equation is:

$$e_a = L_a \frac{di_a}{dt} + R_a i_a + e_b \tag{2}$$

The torque generated by the armature current is proportional to the sum of the inertia and friction torques as follows:

$$T = J \frac{d\omega}{dt} + B\omega = Ki_a \tag{3}$$

Since the load torque is considered a defect in the control system of the linear DC motor system, it is not taken into consideration in Equation (3). The Laplace transforms of Equations (1)-(3) will be as the following equations if all of system's initial conditions assumed zero:

$$E_b(s) = K_b \omega(s) \tag{4}$$

$$E_a(s) = (L_a s + R_a) I_a(s) + E_b(s) \tag{5}$$

$$T(s) = (Js + B)\omega(s) = KI_a(s) \tag{6}$$

Figure 2 represents the structure of a DC motor system and Table 2 presents the simulation parameter values for the studied system [5, 12]. The following is a description of the system's open-loop transfer function:

$$G(s) = \frac{\omega(s)}{E_a(s)} = \frac{K}{(L_a s + R_a)(Js + B) + K_b K} \tag{7}$$

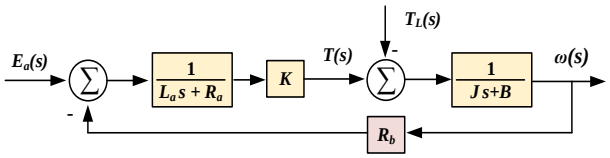

Figure 2. Structure of the DC motor

Table 2. the values of the DC motor's variables

Parameter	Value	Parameter	Value
R_a	0.4	B	0.0022
L_a	2.7	K	0.015
J	0.0004	K_b	0.05

3. FOTID CONTROLLER STRUCTURE

The construction of the TID controller is pretty similar to the structure of the PID controller, except that there is a transfer function just beside the proportional gain as $s^{-1/n}$. The TID controller provides many advantages against the PID controller, including ease of adjustment, more robust disturbance control, and less sensitivity to system parameter changes [13].

In Equations (8) and (9), a TID controller's transfer function and output mathematical equation are presented. K_P, K_I and K_D indicate the proportional, integral, and derivative gain coefficients in these equations, while n is a non-zero constant.

$$TID(s) = \frac{K_P}{s^{1/n}} + \frac{K_I}{s} + sK_D \tag{8}$$

$$U(s) = \frac{K_P}{s^{1/n}} E(s) + \frac{K_I}{s} E(s) + sK_D E(s) \tag{9}$$

The FOTID controller is similar to a FOPID controller and contains two fractional-order parameters of integral (λ) and derivative (μ). This controller has superior disturbance rejection, and it can operate better when uncertainty applies to the system.

The structure of the FOTID controller is displayed in Figure 3. Moreover, the FOTID controller's transfer function and output mathematical equation are shown in Equations (10) and (11). Figure 4 shows the closed-loop block diagram of the DC motor speed control by the FOTID controller.

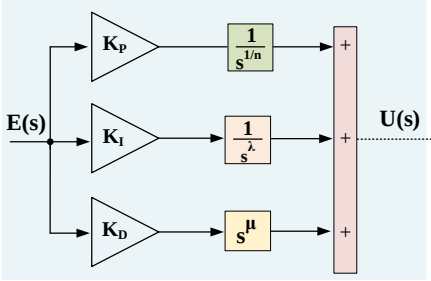

Figure 4. FOTID controller

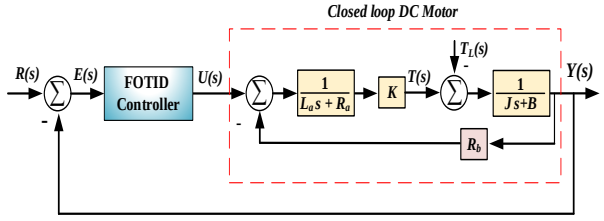

Figure 4. FOTID controller in a DC motor block diagram

4. OBJECTIVE FUNCTION

The ideal tuning of the controller coefficients and the DC motor speed control performance are highly dependent on the objective function. DC motor control systems are typically analyzed based on their transient response characteristics. This response is a reaction to inputs or disturbances while controlling the system. The purpose of developing a powerful controller is to enhance the system response by minimizing time-domain characteristics. Therefore, the objective function should be chosen so that the controller parameters are correctly optimized; and the system's dynamic response has less settling time and least overshoot.

In this article, the integral of squared time multiplied by squared error index (ISTSE) is defined as the objective function, the integral of squared error (ISE), and the integral of time multiplied by squared error (ITSE) are determined as evaluation functions which are given by:

$$J_{ISTSE} = \int_0^{t_{sim}} t^2 e^2(t)dt \tag{12}$$

$$J_{ISE} = \int_0^{t_{sim}} e^2(t)dt \tag{13}$$

$$J_{ITSE} = \int_0^{t_{sim}} te^2(t)dt \tag{14}$$

5. SLIME MOULD ALGORITHM FUNCTION

Slime Mold Algorithm (SMA) is a newly suggested optimization technique based on its behavior modeling. In general, the diffusion and foraging behavior of slime mould has proposed this approach. The SMA focuses on simulating the behavior and morphological changes of the slime mould Physarum polycephalum during foraging rather than modeling the object's whole life cycle. Weights are used in SMA to imitate the regular feedbacks produced by slime mould during foraging [11]. The numerical equation of this method is described in four subsections as following.

5.1. The Stage of Approaching Food

Slime mould can come closer to the food because of the odor in the air. This approaching pattern in mathematical equations is expressed as follows:

$$X(t+1) = \begin{cases} X_b(t) + \upsilon b \cdot (W \cdot X_A(t) - X_B(t)), & r < p \\ \upsilon c \cdot X(t), & r \geq p \end{cases} \tag{15}$$

where, *vb* is a variable with a value between [-*a*, *a*] and *vc* drops from one to zero in a linear way. X_b indicates the highest odor intensity at the individual location. The present iteration is shown by *t*. *X* shows the slime mold's location. X_A and X_B are two slime molds that are randomly selected and slime mold weight is symbolized by *W*. The *p* can be represented as Equation (16):

$$p = \tanh|S(i) - DF|, i = 1, 2, ..., n \tag{16}$$

where the fitness of *X* is symbolized by *S*(*i*) and *DF* shows the best fitness among all iterations. The equation of *a* is determined as follows:

$$a = \arctan h\left(-\left(\frac{t}{t_{\max}}\right)+1\right) \tag{17}$$

where, $t_{\max}$ indicates the greatest iteration number. The equation of *W* is given by:

$$W(SmellIndex(i)) = \begin{cases} 1 + r \cdot \log\left(\frac{bF - S(i)}{bF - wF} + 1\right), & \text{condition} \\ 1 - r \cdot \log\left(\frac{bF - S(i)}{bF - wF} + 1\right), & \text{other} \end{cases} \tag{18}$$

where, *r* defines the random number in the range of [0,1], *bF* indicates the best fitness achieved in the present iterative process and *wF* indicates the worst fitness achieved in the present iterative process [11]. *Smell Index* displays series of fitness values arranged and is expressed as follows:

$$SmellIndex = Sort(S) \tag{19}$$

5.2. The Stage of Wrapping Food

At this stage, the state of contraction and compaction of the mold in the face of food is mathematically simulated. A significant contraction happens in the mold when the food approaches it. The wave produced by the bio-oscillator becomes more robust as the concentration of food contacted by the vein increases, and the cytoplasm flows quicker. The mathematical method for updating the position of slime mold is as follows:

$$X^* = \begin{cases} \text{rand} \cdot (UB - LB) + LB, & \text{rand} < z \\ X_b(t) + \upsilon b \cdot (W \cdot X_A(t) - X_B(t)), & r < p \\ \upsilon c \cdot X(t), & r > p \end{cases} \tag{20}$$

where, *LB* and *UB* indicate the lower and upper search bounds, *rand* and *r* show the random value between [0, 1] and *z* is a parameter with a value between 0 and 0.01.

5.3. The Stage of Grabbling Food

As the quantity of food in the mold varies, the amount of mold shrinkages, and as the volume of food decreases, it causes a wave of oscillation and movement in the mold to look for new food.

The produced wave mainly determines the new location in search of food. Furthermore, *W*, *vb* and *vc* are utilized to simulate the new position of molds.

Slime mold attempts to explore various new regions to discover a higher quality food supply, and if it has got a better food source, it continues to research and select the best food source. The *vb* parameter specifies whether the search for food sources should be stopped or continued. It's also possible that some constraints, such as sunlight and the environment, prevent the search pattern. However, it is possible to find a better-quality food supply without being stuck in the local optimum stage. Figure 5 shows the pseudo-code of the slime mold algorithm.

Algorithm Pseudo-code of slime mould algorithm

Set the population size, maximum iteration;

Initialize slime mould positions X_i $(i=1,2,...n)$;

while ($t \leq$ maximum iteration)

Calculate all slime mould's fitness;

update best fitness, X_b;

calculate W; for each position of search

update *vb*,*vc*,*p*;

update positions; end for

t++; end while

return best fitness,*Xb*

Figure 5. The pseudo code of the SMA

5.4. Design of FOTID Controller

The effective implementation of the FOTID controller in the motor speed control process is dependent on the proper adjusting of the K_P, K_I, K_D, λ, μ and n. Here, the proposed controller parameters is optimized using the SMA [11] to regulate the DC motor speed. This algorithm has significant advantages over genetic (GA), particle swarm optimization (PSO), sine and cosine (SCA) and GWO algorithms in terms of convergence speed, finding better solutions without getting trapped in the local stage.

Figure 6 illustrates the design process of the FOTID controller with the ISTSE index using SMA. The suggested controller parameter's range of adjustments is described in Equation (21). The terms max and min in this relationship denote the parameters' maximum and minimum values, respectively. Table 3 shows the specifications of the SMA used during the design process, and the optimal values of the FOTID and TID controllers are shown in Table 4.

$$\begin{aligned} K_P^{\min} \leq K_P \leq K_P^{\max} \\ K_I^{\min} \leq K_I \leq K_I^{\max} \\ K_D^{\min} \leq K_D \leq K_D^{\max} \\ \lambda^{\min} \leq \lambda \leq \lambda^{\max} \\ \mu^{\min} \leq \mu \leq \mu^{\max} \\ n^{\min} \leq n \leq n^{\max} \end{aligned} \quad (21)$$

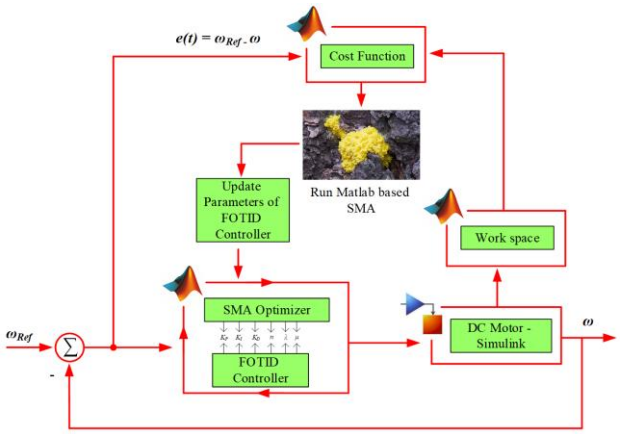

Figure 6. Algorithm-based FOTID controller design process using ISTSE

Table 3. Slime mold algorithm parameters

Parameter	value
Population	50
Iteration	60
Lower bounds of controller parameters	0.001
upper bounds of controller parameters [K_P K_I K_D λ μ n]	[20 20 20 2 1 50]

Table 4. Optimized parameters of controllers

Controller	Parameters					
	K_P	K_I	K_D	λ	μ	1/n
FOTID	18.555	13.798	0.5865	0.879	0.148	0.035
TID	15.789	10.00	0.6780	-	-	0.02

6. SIMULATION RESULTS AND DISCUSSIONS

The studied motor speed control construction is simulated in version 2019b of MATLAB/Simulink software on an intel-corei7/16GB DDR3 system to analyze the performance of FOTID controller. The FOTID controller's performance is compared to the FOPID and TID controller under various scenarios and conditions using the ISE and the ITSE as evaluation functions.

6.1. Case 1

This case intends to analyze the DC motor's step response with FOTID, FOPID, and TID controllers tuned by SMA optimization algorithm. As demonstrated in Figure 7, the FOTID controller has a reduced rise time and improved transient response specifications. In addition, the recommended controller settling time is quicker than other analyzed controllers. Furthermore, Figure 8 presents the percentage improvement in time-domain features in the first case using the FOTID controller vs the TID controller, including overshoot, settling, and rise time. Therefore, it is concluded that the new controller's performance has improved the system's dynamic behavior.

6.2. Case 2

This scenario intends to evaluate the efforts of the suggested algorithm in optimizing the controller coefficients compared to other optimization techniques. The circumstances of this case are precisely the same as the previous scenario. The performance of the SMA is compared with the GWO and PSO based tuned controller.

As demonstrated in Figure 9, the suggested approach could find the controller coefficients properly and get the intended response quicker. Moreover, the outcomes of other algorithms are not very excellent compared to the amount of overshoot and rise time. Therefore, the application of SMA-FOTID in this system is recommended.

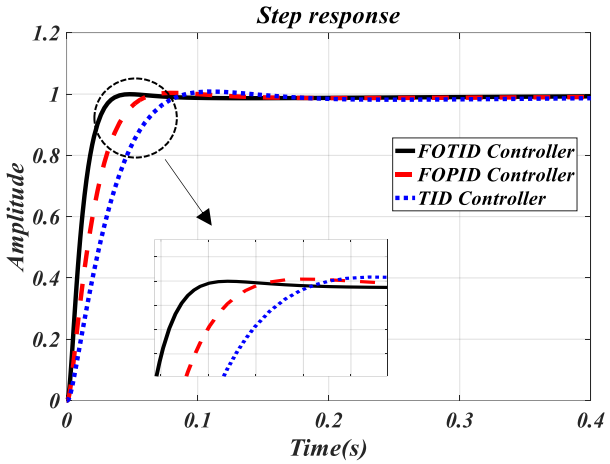

Figure 7. The step response of the DC motor speed in Case 1

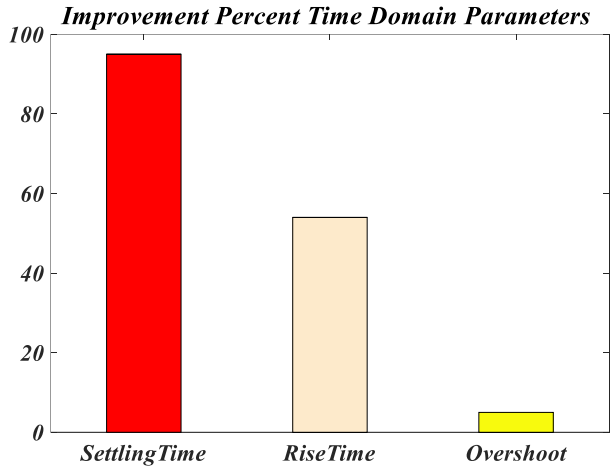

Figure 8. Time response characteristics improvement percentage

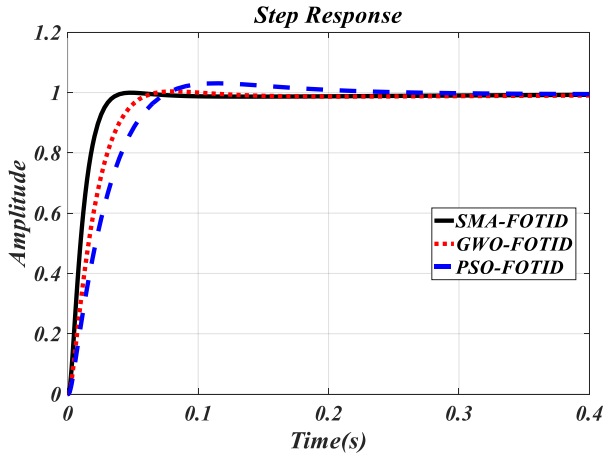

Figure 9. The step response of the DC motor speed in Case 2

6.3. Case 3

In a control system, the effectiveness of the controllers should be compared under parametric uncertainties to analyze them more carefully. In case 3, respectively, 50% and 40% parametric changes are applied incrementally to the parameters of the armature resistance (R_a) and the motor torque constant (K) to demonstrate the strength of the proposed strategy. Figure 10 depicts the second scenario's step response. Despite implementing uncertainties to the parameters of the investigated system, the suggested controller enhances the dynamic performance of the DC motor, and the findings reveal that the suggested FOTID controller effectively decreases the settling time and rise time value in the step response of the system. Similarly, the improvement percentage in settling time with the SMA-FOTID controller compared to the SMA-TID controller is nearly 92%, and the improvement percentage in rise time is 49%. Hence, the suggested method's robustness is verified. Table 5 shows the time response characteristics in the third scenario, including overshoot, settling, and rise time. The findings indicate that the SMA-FOTID controller, as compared to other controllers, can significantly improve the system's dynamic behavior.

6.4. Case 4

This scenario analyzes the system's performance with three FOTID, FOPID, and TID controllers under various step changes, as described in Figure 11. Basically, whenever there is a disturbance in the load torque of the DC motor system, the system's output response should immediately approach zero. Figure 12 represents the system's dynamic response to the step load variation. Therefore, the controller's robustness in minimizing the variations is noticeable. In this situation, it is also shown that the FOTID controller is superior to the others.

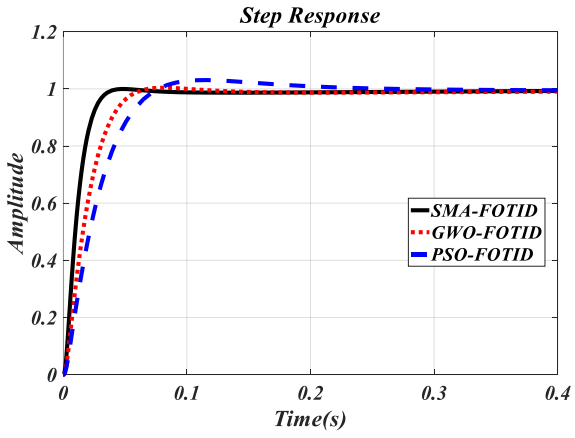

Figure 10. The step response of the DC motor speed in Case 3

Table 5. Comparison of Controllers Time-Domain Performance in the Case 3

Time-domain characteristics		Controllers		
		FOTID	FOPID	TID
Overshoot	ISE	1.036	1.04	1.044
	ITSE	1.031	1.034	1.038
	ISTSE	1.01	1.018	1.026

Time-domain characteristics		Controllers		
		FOTID	FOPID	TID
Rise time	ISE	0.019	0.035	0.042
	ITSE	0.014	0.030	0.037
	ISTSE	0.01	0.015	0.022
Settling time	ISE	0.24	0.29	0.32
	ITSE	0.18	0.21	0.27
	ISTSE	0.1	0.15	0.2

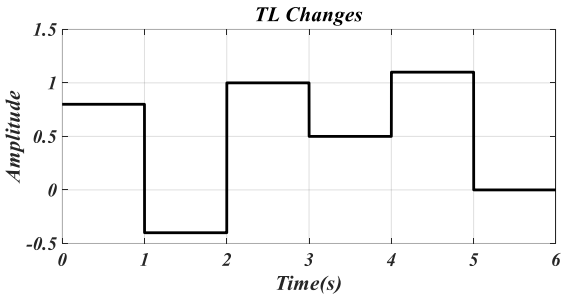

Figure 11. Step changes of the load torque in 6 seconds

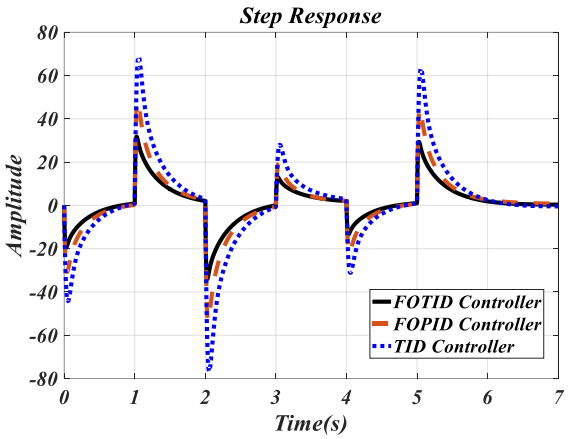

Figure 12. The step response of the DC motor speed in Case 4

6.5. Case 5

This scenario's working mode is the same as the third case, except that some parametric uncertainties are applied at this level. The percentage of parameter changes is indicated in Table 6. The response to the step changes of the fourth scenario is illustrated in Figure 13. The suggested SMA-FOTID controller certainly has the most remarkable performance in regulating deviations regardless of changes in system parameters.

Table 6. DC motor's uncertainty parameters

Parameter	Variation range
R_a	+50%
K	-40%
J	+30%

7. CONCLUSION

This article proposes and investigates a fractional-order TID controller named FOTID for the speed control issue in a DC motor. Because the FOTID controller's functionality is dependent on the appropriate optimization of its coefficients, the SMA is employed to optimize these coefficients and the ISTSE objective function was utilized to determine the best controller coefficients throughout the controller design process.

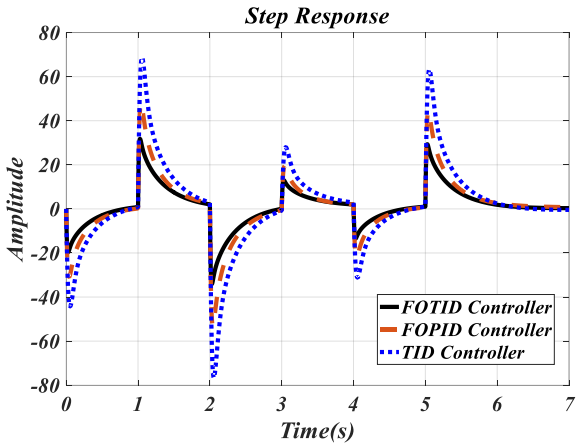

Figure 13. The step response of the DC motor speed in Case 5

The suggested FOTID controller behavior analysis has been performed to evaluate its efficiency by implementing various step inputs to the DC motor system under different scenarios. According to the simulation results, the SMA-FOTID controller can reduce speed deviations to the desired level. Furthermore, the suggested controller results showed greater resilience to system parameter changes (uncertainties). By comparing the FOTID controller with the FOPID and TID controllers, the results of the simulations demonstrate that the suggested controller is highly practical.

REFERENCES

[1] M. Kushwah, A. Patra, "Tuning PID Controller for Speed Control of DC Motor using Soft Computing Techniques-A Review", Advance in Electronic and Electric Engineering, Vol. 4, No. 2, pp. 141-148, 2014. Clerk Maxwell J., A Treatise on Electricity and Magnetism, 3rd ed., Vol. 2. Oxford: Clarendon, pp. 68-73, 1892.

[2] H. Moayedirad, S. Nejad, "Increasing the Efficiency of the Power Electronic Converter for a Proposed Dual Stator Winding Squirrel-Cage Induction Motor Drive Using a Five-Leg Inverter at Low Speeds", Journal of Operation and Automation in Power Engineering, Vol. 6, No. 1, pp. 23-39, 2018.

[3] S. Ekinci, D. Izci, B. Hekimoglu, "PID Speed Control of DC Motor using Harris hawk's Optimization Algorithm", IEEE International Conference on Electrical, Communication and Computer Engineering (ICECCE), pp. 1-6, 2020.

[4] B. Hekimoglu, "Optimal Tuning of Fractional Order PID Controller for DC Motor Speed Control via Chaotic Atom Search Optimization Algorithm", IEEE Access, Vol. 7, pp. 38100-38114, 2019.

[5] J. Agarwal, G. Parmar, R. Gupta, A. Sikander, "Analysis of Grey Wolf Optimizer Based Fractional Order PID Controller in Speed Control of DC Motor", Microsystem Technologies, Vol. 24, No. 12, pp. 4997-5006, 2018.

[6] A. Mishra, N. Singh, S. Yadav, "Design of Optimal PID Controller for Varied System using Teaching-Learning-Based Optimization", Advances in Computing and Intelligent Systems: Springer, 2020, pp. 153-163.

[7] S. Weerasooriya, M.A. El Sharkawi, "Identification and Control of a DC Motor using Back-Propagation Neural Networks", IEEE Transactions on Energy Conversion, Vol. 6, No. 4, pp. 663-669, 1991.
[8] D. Xue, C. Zhao, Y. Chen, "Fractional Order PID Control of a DC-Motor with Elastic Shaft: A Case Study", IEEE American Control Conference, p. 6, 2006.
[9] A. Rawat, M. Azeem, "Speed Control of Brushless DC Motor using Modified Genetic Algorithm Tuned Fuzzy Controller", Current Journal of Applied Science and Technology, Vol. 39, No. 9, pp. 54-64, 2020.
[10] N. Razmjooy, Z. Vahedi, V.V. Estrela, R. Padilha, A.C.B. Monteiro, "Speed Control of a DC Motor Using PID Controller Based on Improved Whale Optimization Algorithm", Metaheuristics and Optimization in Computer and Electrical Engineering, Springer, pp. 153-167, 2021.
[11] S. Li, H. Chen, M. Wang, A.A. Heidari, S. Mirjalili, "Slime Mold Algorithm: A New Method for Stochastic Optimization", Future Generation Computer Systems, Vol. 111, pp. 300-323, 2020.
[12] M. Khalilpour, N. Razmjooy, H. Hosseini, P. Moallem, "Optimal Control of DC Motor using Invasive Weed Optimization (IWO) Algorithm", Majlesi Conference on Electrical Engineering, Isfahan, Iran, 2011.
[13] B.J. Lurie, "Three-Parameter Tunable Tilt-Integral-Derivative (TID) Controller", 1994.

BIOGRAPHIES

Reza Mohajery was born in Ardabil, Iran, in 1998. He received the B.Sc. degree in Electrical Engineering from University of Tabriz, Tabriz, Iran in 2019. Currently, he is a M.Sc. student in the field of Power Electrical Engineering in Technical Eng. Department of University of Mohaghegh Ardabili, Ardabil, Iran. His research interests are about renewable energy, smart grids, power electronics topology, DC Motors, DC-DC Converter control and applications.

Hossein Shayeghi received Ph.D. degree in Electrical Engineering from Iran University of Science and Technology, Tehran, Iran in 2006. He is currently a Professor and the Scientific Director of the Energy Management Research Center, University of Mohaghegh Ardabili, Ardabil, Iran. His research interests are power system control and operation, microgrid and smart grids control and energy management and Fact's device. He has authored and co-authored of 12 book chapters in international publishers and more than 430 papers in international journals and conference proceedings that received in Google Scholar more than 6377 citations with an H-index equal to 40. He has been included in the Thomson Reuters' list of the top one percent of most-cited technical Engineering scientists in 2015-2021, respectively. Also, He is editor-in-chief of Journal of Operation and Automation in Power Engineering and Journal of Energy Management and Technology. He is a senior member of IEEE.

Peyman Zare was born in Ardabil, Iran, in 1995. He received the B.Sc. degree in Biomedical Engineering from Islamic Azad University, Ardabil, Iran, in 2019 and M.S. in Power Electrical Engineering from Mohaghegh Ardabili University, Ardabil, Iran, in 2021. Currently, he is working toward the Ph.D. degree in Power Electrical Engineering at Mohaghegh Ardabili University, Ardabil, Iran. His research interests include marine vessel power systems, renewable energy, microgrid, smart grids, automatic generation control (AGC), load frequency control (LFC).